Supplementary Information of

Application of machine learning to assess the influence of microstructure on twin nucleation in Mg alloys

Biaobiao Yang, Valentin Vassilev-Galindo, Javier Llorca

Published in npj Computational Materials (2024)

Supplementary Figures

Supplementary Figure 1. Difference of textures for AZ31 and Mg-1Al alloy

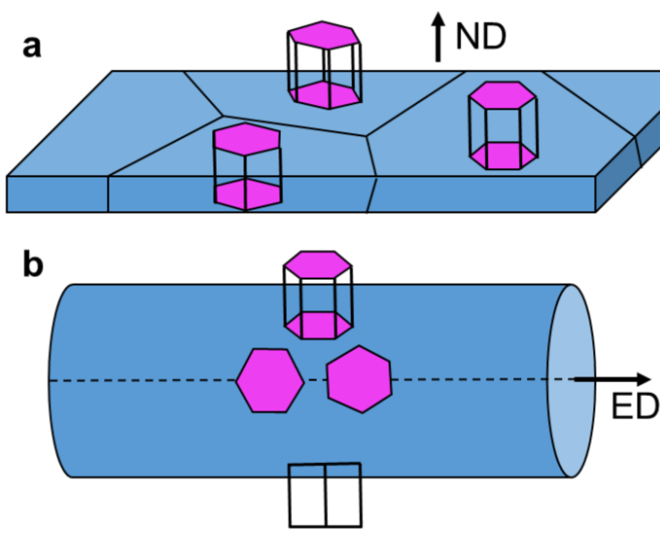

Supplementary Figure 1. Schematic illustration of a) strong basal texture of AZ31 Mg alloy and b) strong prismatic texture of Mg-1Al alloy. ND and ED represents the normal and extrusion directions, respectively.

Supplementary Figure 2. Microstructure of AZ31 Mg alloy

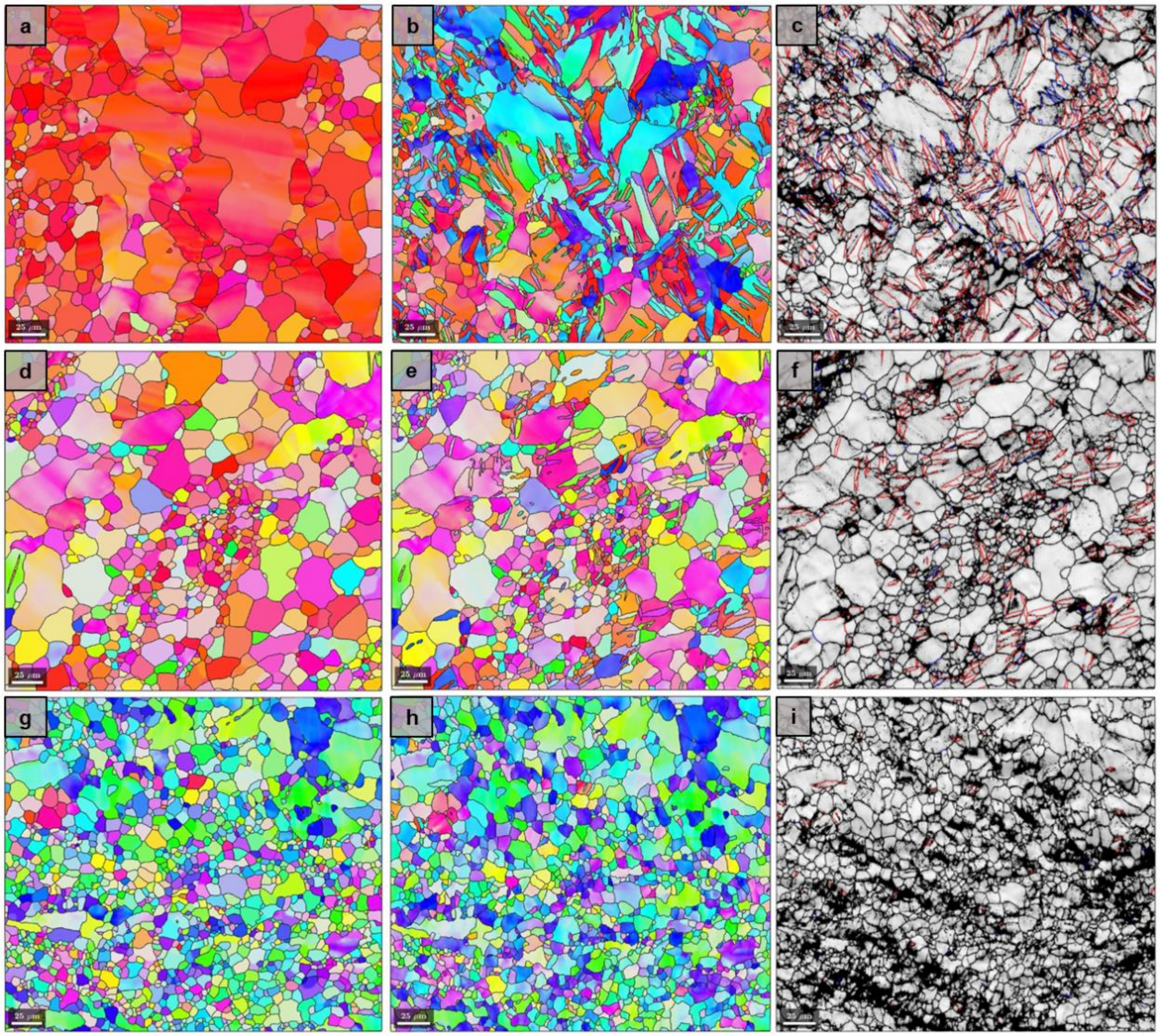

Supplementary Figure 2. Microstructures of samples a-c) S0, d-f) S45, and g-i) S90 before and after deformation. Electron back-scattered diffraction (EBSD) inverse pole figure (IPF) maps in the horizontal direction of samples **a, d, g)** before and **b, e, h)** after deformation. EBSD band contrast (BC) maps of samples **c, f, i)** after deformation. All grain boundaries were overlaid in black. Extension twins and secondary twin boundaries were highlighted in red and blue, respectively, in the BC maps. Note that their identification was performed by measuring the rotation axis - misorientation angle of every boundary. The rotation axis & angle pairs for extension twin and secondary twin are $\langle 2\bar{1}\bar{1}0\rangle$ & 86.30°, and $\langle 1\bar{1}00\rangle$ & 60.00°, respectively.

Supplementary Figure 3. Microstructure of Mg-1Al alloy

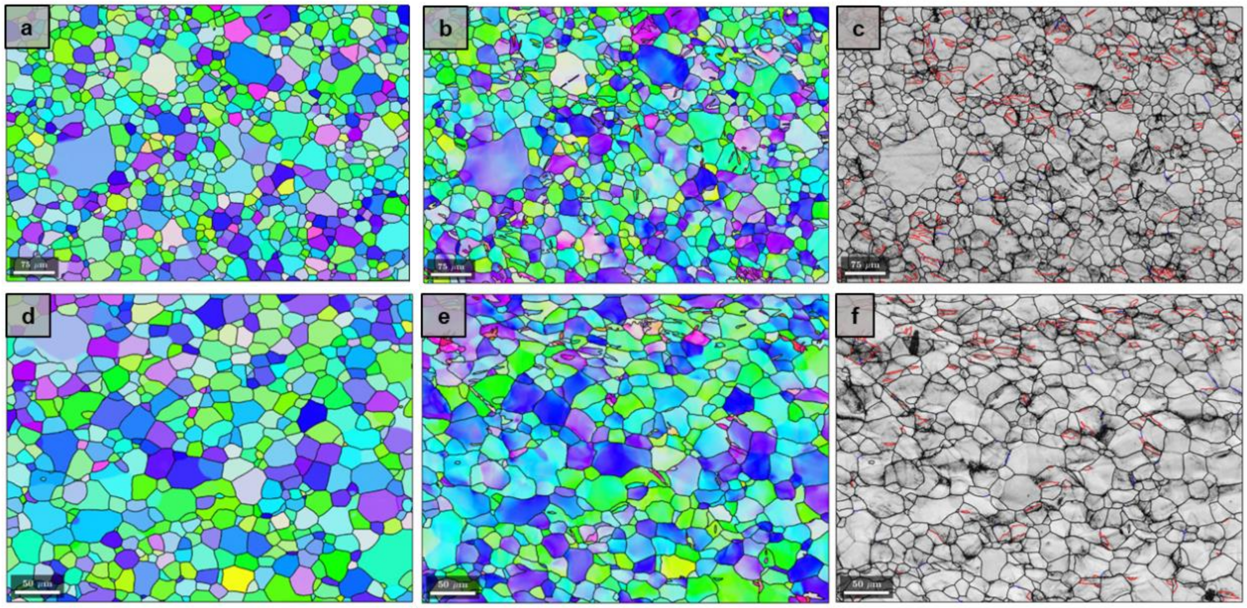

Supplementary Figure 3. Microstructures of Mg-1Al samples a, d) before and after deformation up to b, c) 6%, and e, f) 10% engineering strains. The reference direction of EBSD IPF maps is the extruded direction. All grain boundaries were overlaid in black. Extension twin and secondary twin boundaries were highlighted in red and blue, respectively, in the BC maps. Note that their identification was performed by measuring the rotation axis - misorientation angle of every boundary. The rotation axis & angle pairs for extension twin and secondary twin are $\langle 2\bar{1}\bar{1}0 \rangle$ & 86.30°, and $\langle 1\bar{1}00 \rangle$ & 60.00°, respectively.

Supplementary Figure 4. Active slip analysis using grain reference orientation deviation [1]

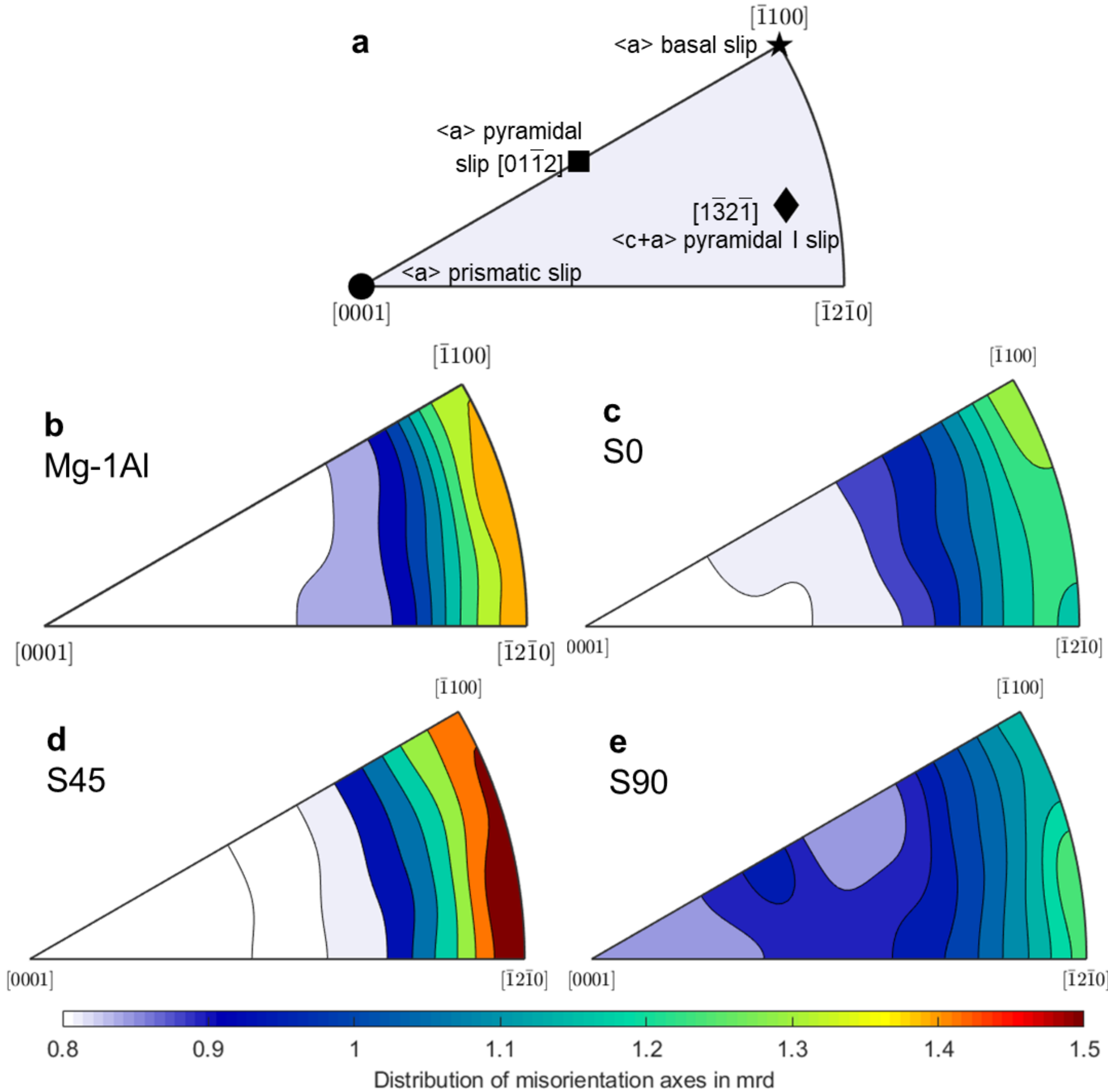

Supplementary Figure 4. Slip behavior analysis of deformed Mg-1Al (9.5% true strain) and AZ31 alloy (6% true strain). a) Rotation axes associated with dislocation slip along different systems in hexagonal close-packed (HCP) Mg. Evolution of the distribution of intragranular misorientation axes in the crystal coordinate system (expressed in multiples of random distribution, mrd) of Mg alloy during tensile deformation along different directions. **b)** Mg-1Al, **c)** S0, **d)** S45, and **e)** S90.

Supplementary Figure 5. Luster-Morris geometric compatibility factor (*m'*)

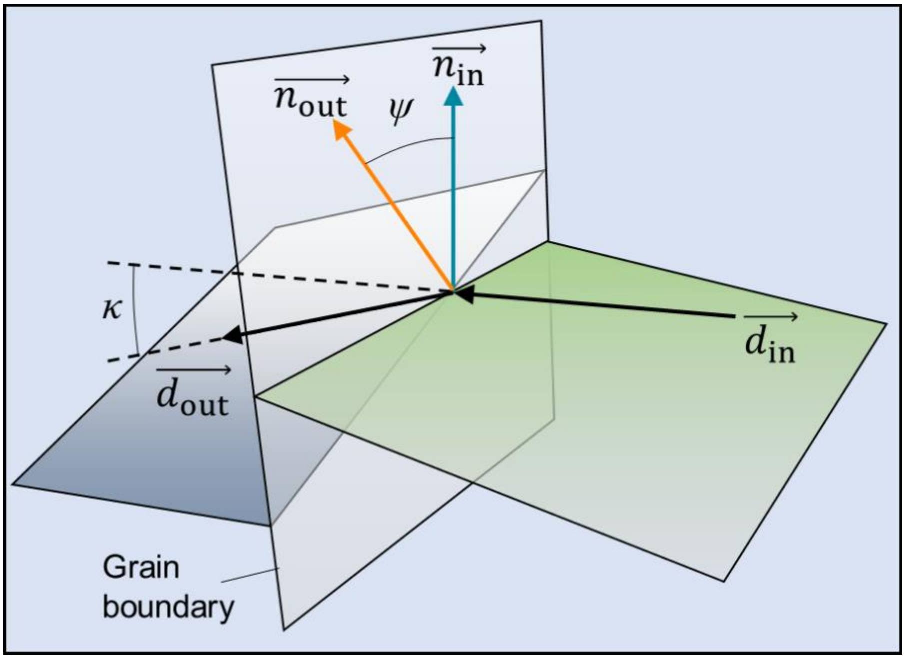

Supplementary Figure 5. Geometrical factors to define the Luster-Morris parameter (*m'*) at a grain boundary (GB).

Supplementary Methods. Optimal hyperparameters of the Bayesian network models

1) AZ31

learningMethod = 'GHC'

discretizationNbBins = 3

discretizationStrategy = 'quantile’

UsePR = False

2) AZ31 MB (for both *Max_deltaBSF* and *S_SF1*)

learningMethod= 'MIIC'

discretizationNbBins = 3

discretizationStrategy = 'quantile'

UsePR = False

3) AZ31 [T_SF1 < 0.16]

learningMethod = 'MIIC'

discretizationNbBins = 3

discretizationStrategy = 'quantile'

UsePR = True

4) Mg-1Al

learningMethod = 'Tabu'

discretizationNbBins = 3

discretizationStrategy = 'quantile’

UsePR = False

5) AZ31 [*T_SF1* < 0.16] MB

learningMethod = 'NaiveBayes'

discretizationNbBins = 3

discretizationStrategy == 'quantile'

UsePR = False

6) Mg-1Al MB

learningMethod = 'TAN'

discretizationNbBins = 3

discretizationStrategy = 'quantile'

UsePR = False

7) AZ31 [*T_SF1* < 0.16] MB (*Min_deltaGs)*

learningMethod = 'MIIC'

discretizationNbBins = 3

discretizationStrategy = 'quantile'

UsePR = False

8) Mg-1Al MB (*Grain_size*)

learningMethod = 'Chow-Liu'

discretizationNbBins = 3

discretizationStrategy = 'quantile'

UsePR = True

Supplementary Reference

1. Tong, V., Wielewski, E. & Britton, B. Characterisation of slip and twinning in high rate deformed zirconium with electron backscatter diffraction. Preprint at https://doi.org/10.48550/arXiv.1803.00236 (2018).